

Reprinted from

Canadian Journal of Chemistry

Composition of Tetrahydrofuran Hydrate
and the Effect of Pressure on the
Decomposition

S. R. GOUGH AND D. W. DAVIDSON

Volume 49 • Number 16 • 1971

NRCC No. 12002

Published by The National Research Council of Canada

NOV 3 1971

Composition of Tetrahydrofuran Hydrate and the Effect of Pressure on the Decomposition¹

S. R. GOUGH AND D. W. DAVIDSON

Division of Chemistry, National Research Council of Canada, Ottawa, Canada

Received March 12, 1971

The decomposition temperature of the structure II clathrate hydrate of tetrahydrofuran has been followed to pressures above 3 kbars, where the hydrate is found to decompose incongruently in the regions of stability of ices III and II, with no evidence of formation of a denser hydrate. From measurements of liquid solution densities and of volume changes at hydrate decomposition the density of the hydrate was obtained. Comparison with the X-ray lattice dimension indicates that at least 98% of the large cages are occupied, the principal uncertainty being in the lattice parameter. A similar treatment is made of Tammann and Krige's data (23) for chloroform hydrate. Analysis of the results of 18 composition determinations of structure II hydrates shows no statistical evidence of departure from the ideal composition of 17 mol of water per mol of hydrate former.

La température de décomposition du clathrate hydraté de structure II du tétrahydrofurane a été suivie jusqu'à des pressions supérieures à 3 kbar; il a été trouvé que dans ces régions de stabilité des glaces III et II l'hydrate se décompose d'une façon aberrante sans preuve de formation d'un hydrate plus dense. A partir des mesures de densité des solutions liquides et des changements de volume à la décomposition de l'hydrate, il a été possible d'obtenir la densité de l'hydrate. La comparaison avec la dimension du réseau obtenu par rayons X indique qu'au moins 98% des grandes cages sont occupées, l'incertitude principale étant dans le paramètre réticulaire. A partir des données de Tamman et Krige une analyse similaire est effectuée pour le chloroforme hydraté. Les analyses des résultats se rapportant à 18 déterminations de composition d'hydrates ayant la structure II ne montrent aucune preuve statistique d'écart par rapport à la composition idéale de 17 mol d'eau par mole de générateur d'hydrate.

Canadian Journal of Chemistry, 49, 2691 (1971)

Among the diverse molecules now known to form "gas hydrates" of von Stackelberg's structures I and II (1) are a number of ethers and ketones which are distinguished from the classical gas-hydrate formers by their solubility in water and by the possibility of hydrogen bonding with the host water molecules of the clathrate structures. Ethylene oxide (2, 3) and trimethylene oxide (4) form hydrates of type I. Structure II hydrates are formed by dimethyl ether (1), by trimethylene oxide, tetrahydrofuran, 2,5-dihydrofuran, propylene oxide, and 1,3-dioxolane (4, 5) and by acetone (6, 7) and cyclobutanone (5, 8). With the exception of the study by Glew and Rath (9) of the variable composition of ethylene oxide hydrate, there appears to be no accurate information about the degree of occupancy of the cages or the heat of formation of these hydrates.

Trimethylene oxide (4) and acetone (8) hydrates decompose incongruently. Of the other structure II hydrates only tetrahydrofuran hydrate melts appreciably above 0 °C. This hydrate is

therefore most easily distinguished from ice and has been chosen for further study.

Tetrahydrofuran hydrate was first reported by Palmer (10) who found from melting point *vs.* concentration curves a composition of between 13 and 16 molecules of water per molecule of tetrahydrofuran (THF), with a probable formula of THF·14H₂O. Erva (11) obtained a congruent melting point of 4.38 °C at an approximate composition of THF·16H₂O. Several nugatory irregularities in the melting points of solutions of higher THF content were interpreted as peritectic points of lower hydrates (11) or in terms of discrete association complexes in liquid solution (12). They are more likely to be related to the incorporation of different amounts of air in different hydrate samples.

Among several indirect methods (13) of determining the composition of clathrate hydrates, one which is particularly applicable to the hydrates of water-soluble molecules depends on comparison of measured hydrate density with the composition-dependent density calculated from the X-ray unit cell dimensions. Glew and Rath (9) have used the results of flotation mea-

¹NRCC No. 12002.

measurements of the density of ethylene oxide hydrate in conjunction with the lattice parameter to obtain compositions of this hydrate. We have determined the density of THF hydrate from measurements of the volume change at hydrate decomposition and of the density of the liquid solution. Volume, capacitance, and thermal-analysis measurements were made to high pressures to determine the effect of pressure on the hydrate-solution equilibrium and to look for evidence of a transformation of the hydrate to a denser crystallographic form. Heats of formation of the hydrate were estimated from the results.

Experimental Methods

The initial measurements were made to define the region of stability of THF hydrate in the pressure-temperature plane. The decomposition of the hydrate was followed by the capacitance, conductance, and volume changes which accompanied increase of temperature or pressure through the decomposition region. Some experiments were also made with pressure decreasing. The cell used was that previously described (Fig. 1(b) of ref. 14), with essentially the same methods of control and measurement of temperature and pressure. The electrical measurements were normally made at 20 kHz. The driving piston was coupled to a slow-speed motor to effect rotational oscillation through $\pm 4^\circ$ and thereby to reduce piston friction. Volume changes were measured in terms of displacement of this piston which was monitored to 10 μm . by a dial gauge.

Solutions were prepared from conductivity water and THF which had been distilled over calcium hydride. Analysis by vapor phase chromatography showed the THF to contain 0.1% of volatile impurity. Compositions ranged from THF \cdot 17.0H $_2$ O to THF \cdot 16.8H $_2$ O. Hydrate was normally prepared by cooling to below 0 $^\circ\text{C}$ and conditioning at +2 $^\circ\text{C}$ and 1 atm for about 12 h, followed by over-night conditioning at a temperature and pressure near the starting point of the decomposition measurements.

Most hydrate samples showed relatively small capacitance and volume changes associated with the melting of ice: conductance was particularly sensitive to such eutectic melting. For these samples both ice and hydrate melting data were recorded. Since the measuring thermocouple was outside the pressure vessel (14) in these measurements, melting points were taken as the temperatures at the onset of melting, upon which there was usually agreement to within a few tenths of a degree among the parameters measured. Figure 1 illustrates such warming curves. Measurements with varying pressure refer to equilibrated temperatures, but the transitions tended to occur over a range of pressure and to show hysteresis when the pressure change was reversed (Fig. 2). Nevertheless, the hydrate and ice melting points appear to have been generally defined to better than 1 $^\circ$ and 100 bars.

Considerably more accurate determination of the variation of hydrate decomposition temperature (and

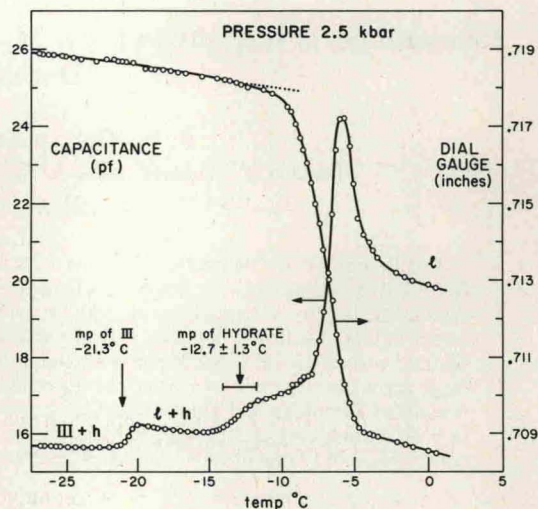


FIG. 1. Illustration of capacitance and volume changes at temperatures of phase changes in the THF-water system.

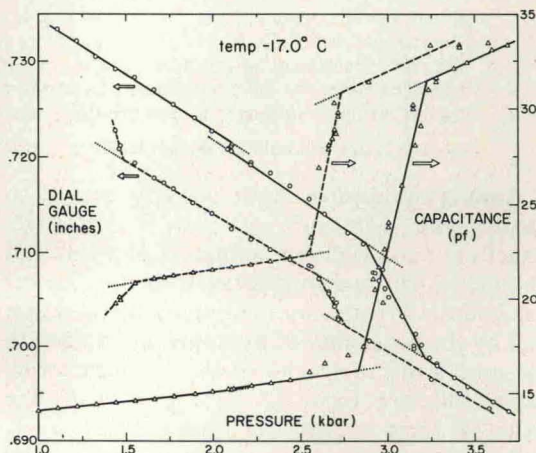


FIG. 2. Capacitance and volume changes at pressures of hydrate decomposition (pressure increasing, solid lines) and formation (pressure decreasing, broken lines).

volume) with pressure to 1400 bars was realized by insertion of a calibrated Chromel-Alumel thermocouple into the center of the sample, the insulated leads, swaged in a stainless steel tube, being brought out through the lower electrode and piston. Since the presence of the thermocouple interfered with the electrical measurements, the decomposition temperature was determined from the dilatometric and thermal (temperature vs. time) measurements only, as the mid-points of the volume changes or of the thermal steps. An example is shown in Fig. 3. All such measurements were made with a sample of composition THF \cdot 16.69H $_2$ O at a heating rate of about 0.2 $^\circ$ /min.

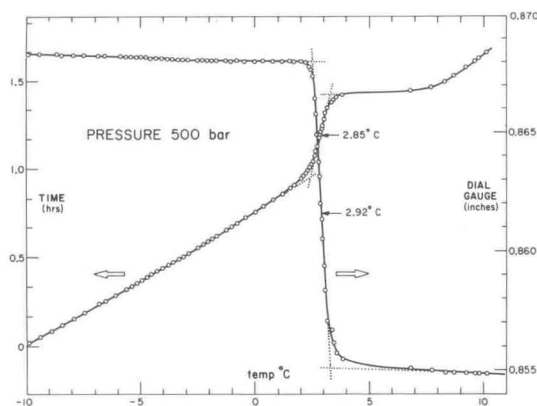


FIG. 3. Example of determination of temperature and volume change of decomposition of THF hydrate.

Densities of liquid solutions near 4 °C were measured with a quartz pycnometer of 11 ml capacity designed after Kirshenbaum (15) and calibrated with mercury and water at 4 °C. The bath temperature was regulated to ± 0.01 °C and measured with a platinum resistance thermometer.

Results

Solution Densities

The densities of a solution of composition THF·16.98H₂O at four temperatures near the hydrate decomposition point at 1 atm are given in Table 1, along with a single measurement of a more dilute solution. The accuracy is considered to be ± 0.00003 g/cm³, with a relative accuracy with respect to temperature change of the first solution of ± 0.00001 g/cm³. These data are sufficient to define the dependence on composition and temperature necessary for determination of the density at the decomposition temperature and over the range of possible hydrate compositions considered below. The appreciable decrease of density with increase of temperature is not surprising, since Wada and Umeda (16) found that THF lowers the temperature of maximum density of water. Extrapolation of their results suggests this temperature to be about -15 °C for a composition of THF·17H₂O.

Phase Equilibria of THF Hydrate

Figure 4 (heavy line) shows the region of stability of THF hydrate. At pressures below 3.05 kbar the hydrate melts congruently to a liquid of greater density, the curvature of the temperature-pressure line being determined by the larger compressibility and thermal contraction of the liquid. This part of the hydrate de-

TABLE 1. Densities of THF solutions

Composition	Temperature (°C)	Density (g/cm ³)
THF·16.98H ₂ O	4.03 ₅	0.99730
	4.13 ₃	0.99726
	4.31 ₁	0.99719
	4.67 ₅	0.99706
THF·17.99H ₂ O	3.98 ₀	0.99768

composition curve intersects the freezing curve of ice III in the presence of liquid of hydrate composition at -19.8 °C and 3.05 kbar. At higher pressures the hydrate (h) "melts" incongruently to give ice III and a peritectic liquid (l), the dependence of decomposition temperature on pressure becoming increasingly great as ice III is formed in greater proportion. The decomposition curves in this region were not well enough defined to distinguish between the h → III + l and h → V + l curves, ice V (as shown by its melting behavior) having been obtained in most pressurizing runs within the region of stability of ice III. When the ice formed is V, the melting of the hydrate remains congruent to about -21.4 °C and 3.12 kbar. At lower temperatures the equilibrium decomposition is to ice II and THF-rich liquid. Dielectric studies (to be published elsewhere) show the hydrate to be stable to at least 3.5 kbar at -62 °C.

There was no evidence of formation of a denser hydrate.

Melting of Ice in the Presence of THF

Over its full range, the curve corresponding to eutectic melting of ice I in the presence of hydrate (Fig. 4) lies about 1° below the melting curve of ice I given by Bridgman (17). This suggests that the eutectic composition shows little variation over this pressure range from its value (0.9 mol% THF (11)) at 1 bar and that the partial molar volume of water (V_1) in the eutectic liquid is not much different from the molar volume of pure water (V_1^0) at the same pressure. The increasing depression of the freezing point of ice III with increase of pressure corresponds to increasing THF content of the eutectic solution, which reaches the hydrate composition at the intersection with the hydrate melting curve. On the other hand, the increasing depression of the freezing point of ice V, 5° at 6.2 kbar, is due to an increasing value of $V_1^0 - V_1$, where V_1 refers to the liquid of the same composition as the hydrate.

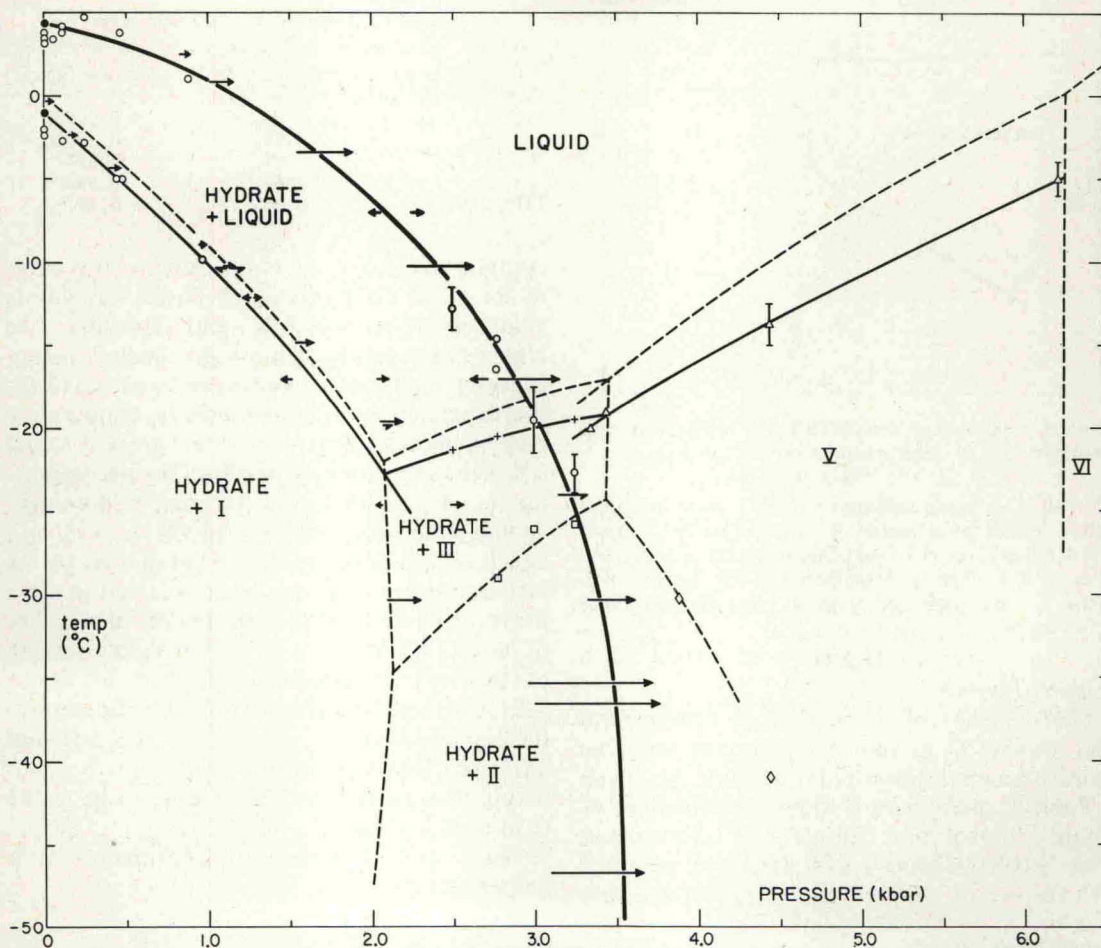


FIG. 4. Phase diagram of the THF-water system. The heavy line is the decomposition curve of THF hydrate, light lines are water-rich eutectic points (to left of heavy line) or melting points of ice in the THF·17H₂O system (to right), and broken lines are Bridgman's phase boundaries in the water system.

Dependence of Decomposition Temperature on Pressure

The decomposition temperature of THF·16.69-H₂O given by the mid-points of the thermal steps in the temperature *vs.* time curves were measured at 17 pressures between 1 and 1400 bars. The results (Fig. 5) are given, to a standard deviation (σ) of 0.080°, by

$$[1] \quad t(^{\circ}\text{C}) = (4.126 \pm 0.035) \\ - (2.280 \pm 0.139) \times 10^{-3} P \\ - (1.150 \pm 0.112) \times 10^{-6} P^2$$

where P is the pressure in bars.

The temperatures at the mid-points of the

corresponding volume changes were measured at 14 pressures (Fig. 5) and are given, with $\sigma = 0.093^{\circ}$, by

$$[2] \quad t(^{\circ}\text{C}) = (4.279 \pm 0.082) \\ - (2.375 \pm 0.259) \times 10^{-3} P \\ - (1.169 \pm 0.176) \times 10^{-6} P^2$$

No reduction of variance was achieved by the inclusion of terms in P^3 in the least squares analyses.

The mid-points of the decomposition curves were chosen for greatest accuracy of the pressure dependence of the melting points. Equations 1 and 2 are expected to underestimate the melting

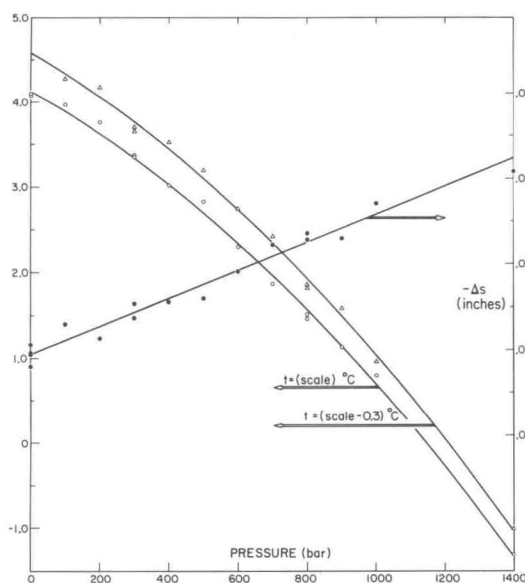


FIG. 5. Pressure dependence of decomposition temperature from thermal (O) and volume (Δ) measurements and of change of piston displacement (\bullet) at decomposition. (The decomposition temperatures from volume measurements are displaced upward by 0.3 °C.)

point of the hydrate at 1 bar because of the central position in the sample of the measuring thermocouple. This appears to be less true of eq. 2, possibly because of some lag of the piston behind the change of volume.

The linear coefficients in eqs. 1 and 2 may be combined to yield

$$[3] \left(\frac{dt}{dP} \right)_{P \rightarrow 0} = -(2.301 \pm 0.122) \times 10^{-3}$$

degrees per bar, the error quoted, like those of eqs. 1 and 2, being the standard error.

Volume Change of Hydrate Decomposition

Seventeen measurements of the change of dilatometer gauge reading for THF·16.69H₂O at pressures between 1 and 1400 bars (Fig. 5) gave

$$[4] \Delta s \text{ (in.)} = -(0.00972 \pm 0.00021) - (8.22 \pm 0.35) \times 10^{-6} P$$

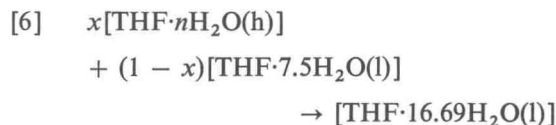
The value of σ (0.00057 in.) was scarcely improved, and the constant term hardly affected, by inclusion of a term in P^2 .

Division of Δs for $P = 1$ bar, by the length of the column of liquid solution at 4.4 °C gave

$$[5] \Delta v/v = \Delta s/s = -(0.01470 \pm 0.00034)$$

for the relative change of volume. From Table 1 the density of liquid THF·16.69H₂O at 4.4 °C may be taken as $0.99705 \pm 0.00004 \text{ g cm}^{-3}$, whence the change of volume is $-5.496 \pm 0.129 \text{ cm}^3$ per mol of THF·16.69H₂O.

This volume change is not quite the desired volume change for congruent melting of 1 mol of hydrate of composition THF· n H₂O, since $n > 16.69$. Some melting of the hydrate occurs over the whole temperature between the THF-rich eutectic temperature and the final melting point. Examination of the volume *vs.* temperature curves shows that a contribution to the measured volume change is first detected about 1° below the temperature of final melting. Erva's data (11) show the liquid composition to be THF·7.5H₂O at this temperature. The measured volume change then corresponds to



where $x = 9.19/(n - 7.5)$ is the fraction of THF present in the hydrate at the onset of melting.

Reaction 6 may be considered as the sum of the processes of melting x mol of hydrate and of mixing x mol of liquid THF· n H₂O with $(1-x)$ mol of liquid THF·7.5H₂O. The volume change of mixing is zero for an ideal solution. The density measurements of THF-water solutions at 25 °C by Critchfield *et al.* (18) give zero for this volume change, with n near 17, to within the experimental accuracy of 0.02%. We ascribe the whole of the measured volume change to the melting of x mol of hydrate and put for the melting of 1 mol

$$[7] \Delta V(h \rightarrow l) = \frac{-5.496}{x} \pm \frac{1}{x} \sqrt{30.25(1-x)^2 + 0.0640}$$

The error estimate² has been conservatively written to include an uncertainty in the correction ($1/x$) of the order of magnitude of the correction itself and the original standard error of the measured volume change has been expanded to the 95% confidence level.

²The error in x is assumed to be $x(1-x)$ and in the measured volume change $1.96 \times 0.129 \text{ cm}^3$.

Hydrate Composition

The molar volume of $\text{THF} \cdot n\text{H}_2\text{O}(l)$ at 4.4° may be written as

$$[8] \quad V(l) = \frac{72.10 + 18.015n}{0.99716 + 0.000364(n - 16.98)} \text{ cm}^3$$

and that of the solid hydrate as

$$[9] \quad V(h) = \frac{Nna^3}{136} \text{ cm}^3$$

where N is Avogadro's number and a is the dimension of the cubic unit cell which contains 136 water molecules. Unfortunately, a is not accurately known at the decomposition temperature of the hydrate. Von Stackelberg and Meuthen's value (2) of 17.18 \AA at -10°C appears to be uncertain by as much as 0.10 \AA . The more accurate values of Sargent and Calvert (5), *viz.*, $17.13 \pm 0.03 \text{ \AA}$ at -163°C and two values of 17.170 ± 0.004 and $17.162 \pm 0.007 \text{ \AA}$ at -137°C (the errors are σ 's), refer to much lower temperatures. The values (5) for the closely related hydrate of dihydrofuran, almost identical with those of THF hydrate at -137°C , include $17.22 \pm 0.01 \text{ \AA}$ at -40°C . Extrapolation of the combined data for THF and dihydrofuran hydrates to 4°C gives 17.24 \AA , to which we assign a maximum uncertainty of $\pm 0.03 \text{ \AA}$.

In Fig. 6 volumes given by eq. 7 and by the difference between eqs. 8 and 9 are plotted against n for values of a between 17.21 and 17.27 \AA .

The most probable value of n is 16.86 . For the

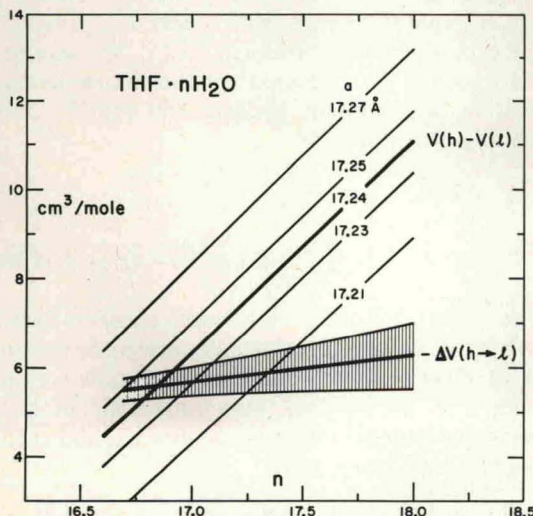


FIG. 6. Dependence of volume change at decomposition on composition of THF hydrate.

range of lattice parameters allowed, values between about 16.4 and 17.5 are formally permitted. It is unlikely, however, that THF (maximum diameter 5.9 \AA (2)) can occupy the small cages of free diameter 4.9 \AA and therefore that n is less than 17 . It may also be noted that $a = 17.21 \text{ \AA}$, for which n is 17.34 ± 0.20 , is much less likely than $a = 17.23 \text{ \AA}$, with $n = 17.01 \pm 0.16$. We conclude, at about the 90% confidence level, that at least 98% of the large cages are occupied.

Effect of Air on Hydrate Properties

Under the conditions of our experiments, in which the only air present was that initially dissolved in the liquid, the effect of air on the volume changes discussed above may be shown to be negligible. Saturation with air at 1 atm affects the density of liquid water only in the sixth decimal place (19) and therefore may be assumed to have a negligible effect on the density of the THF solution. If the air present in the solution (assumed to be the amount soluble in water at 4°C) is entirely taken into the small cages of the hydrate, the hydrate density is increased by 0.000034 g/cm^3 and the volume change of melting reduced by only $0.013 \text{ cm}^3/\text{mol}$.

It is well-known that some hydrates grown in the presence of air incorporate large quantities of air in their cages, with a consequent increase of stability (see refs. 13 and 20, for example). A simple experiment showed this to be true of THF hydrate. A sample of $\text{THF} \cdot 16.79\text{H}_2\text{O}$ was slowly frozen and conditioned in an ice bath for several hours. The warming curve obtained in an air-jacketed glass vessel showed the great bulk of the sample to melt at 4.45°C . With further warming the remaining crystals gradually melted with the evolution of air bubbles and only completely disappeared at 5.0°C . It is likely that the presence of air accounts for Palmer's report (10) of two maximum melting points at 5.07 and 5.37°C . The available data suggest that the melting point of THF hydrate containing little or no air lies at $4.4 \pm 0.1^\circ\text{C}$.

Heats of Decomposition

The enthalpy change of congruent melting at negligible pressure is given by

$$[10] \quad \Delta H(h \rightarrow l) = \frac{T \Delta V(h \rightarrow l)}{\left(\frac{dt}{dP}\right)_{P \rightarrow 0}}$$

The pressure coefficient of the melting point is

TABLE 2. Enthalpies of decomposition of THF hydrate

Decomposition	Temperature (°C)	ΔH (kcal/mol)
h \rightarrow l	4.4	16.7 \pm 1.9
h \rightarrow l ₁ + l ₂	4.4	19.5 \pm 2.0
h \rightarrow l ₁ + g	4.4	27.1 \pm 2.0
h \rightarrow l ₁ + g	0	26.5 \pm 2.1
h \rightarrow l + g	0	2.1 \pm 2.1

given by eq. 3. With $\Delta V(h \rightarrow l) = -5.8 \pm 0.3$ cm³, $\Delta H(h \rightarrow l) = 16.7 \pm 1.9$ kcal/mol, at about the 95% confidence level.

We have crudely measured the heat of mixing of 1 mol of THF and 17 mol of water at a mean temperature of 4 °C, and found $\Delta H(l_1 + l_2 \rightarrow l) = -2.8 \pm 0.2$ kcal. This value is consistent with values read from Erva's figure (21), viz., -2.25 and -2.60 kcal for mixing at 25 and 15 °C, respectively. The heat of vaporization of liquid THF at 4.4 °C is found from the vapor pressure equation (22) to be $\Delta H(l_2 \rightarrow g) = 7.6 \pm 0.1$ kcal/mol. These quantities, together with estimates of specific heats between 4.4 and 0 °C, give the enthalpy changes shown in Table 2.

Discussion

Chloroform Hydrate

The only comparable study of the volume change of decomposition of a structure II hydrate appears to be that of Tammann and Krige (23), who measured the volume change and temperature of decomposition of chloroform hydrate to the sparingly miscible liquids at pressures to 2 kbar. Analysis of their data gives, with $\sigma = 0.00144$ cm³/g,

$$[11] \quad \Delta v = (0.01956 \pm 0.00174) \\ - (5.547 \pm 0.470) \times 10^{-5} P \\ + (1.0353 \pm 0.2476) \times 10^{-8} P^2$$

for the change in volume per gram of hydrate. These volume changes were measured indirectly from the changes of pressure at decomposition and were corrected (23) for the considerable amounts of excess water present. From eq. 11, $\Delta V(h \rightarrow l_1 + l_2)$ per mol of hydrate at 1 bar (and about 2 °C) may be written as a function of n .

The solubility at 2 °C of chloroform in water is only 0.96 and of water in chloroform only 0.02 weight % (24). Little error is introduced by assuming additivity of molar volumes in these dilute solutions:

$$[8'] \quad V(l_1 + l_2) = \frac{119.39}{1.5222} + \frac{18.015n}{0.999947}$$

where the density of chloroform is from Timmermans (25). $V(h)$ is given by eq. 9 with $a = 17.33 \pm 0.10$ Å (26).

The volume differences for chloroform hydrate are shown in Fig. 7. The uncertainty shown for $\Delta V(h \rightarrow l_1 + l_2)$ is double the standard error of the constant term in eq. 11.

The most probable value of n is 17.25, but a value as high as 19.0 cannot be definitely excluded because of the large uncertainty of the lattice parameter. Conversely, if, as there is good reason to assume (see below), the large cages are at least 98% occupied, the value of a is defined between 17.30 and 17.37 Å.

The pressure-dependence of the decomposition temperature of chloroform hydrate was not measured (23) with sufficient accuracy to permit a useful estimation of $\Delta H(h \rightarrow l_1 + l_2)$ from eq. 10. This quantity was found to be 22.9 kcal/mol by a calorimetric study made in 1885 (27). Addition of the heat of vaporization of chloroform at 2 °C gives $\Delta H(h \rightarrow l_1 + g) \approx 30.7$ kcal/mol.

Critical Decomposition Temperatures of Structure II Hydrates

For THF and chloroform hydrates the decomposition temperature is highest in the absence of externally-applied pressure. The melting tempera-

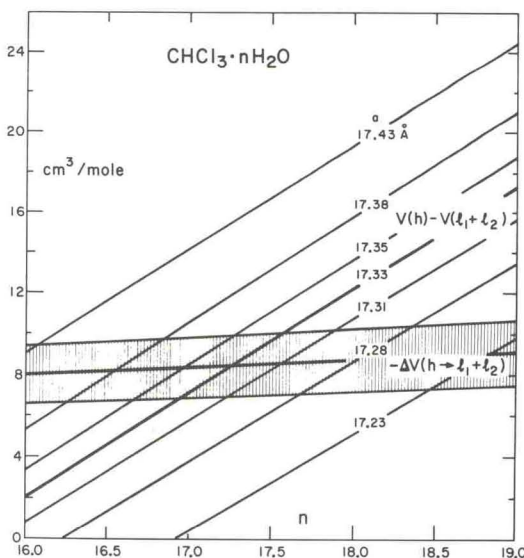


FIG. 7. Dependence of volume change at decomposition on composition of chloroform hydrate.

TABLE 3. Composition of structure II hydrates*

Hydrate	ΔH_1 (h \rightarrow l ₁ + g) (kcal/mol)	ΔH_2 (h \rightarrow I + g) (kcal/mol)	From $\Delta H_1 - \Delta H_2$		From effect of NaCl		Direct analysis <i>n</i>
			<i>n</i>	<i>w</i>	<i>n</i>	<i>w</i>	
SF ₆	29.57	5.14	17.02(33)	3			
Cyclopropane (Deuterate)	29.2 32.37	6.42 6.44	15.87(34) 17.18(35)†	1 3	17.05(34)	3	
<i>n</i> -Propane	32.1	6.34	17.94(36)	1	17.9 (37)	1	19.7(38)
Isobutane	30.5	5.45	17.45(39)	2	17.50(39)	2	17.1(40)
CH ₃ I	31.4	7.3	16.79(13)	1			
CHCl ₃	30.7‡		17.25§	1			18 (27) 17.7(31)
CHCl ₂ F	32.72	8.51	16.86(41)	2	16.80(42)	2	
CCl ₃ F	35.45	11.57	16.63(42)	0			
CCl ₂ F ₂	30.14	7.79	15.57(42)	0			
CBrClF ₂	32.567 31.86(43)	8.254	16.94(29)	4	16.57(43)	2	
CBrF ₃	29.42	6.99	15.62(42)	0			
CH ₃ CH ₂ Cl	31.9	8.7	16.16(13)	1			
CH ₃ CClF ₂	31.11	7.49	16.45(44)	1	17.18(44)	2	
C ₄ H ₈ O	27.1‡		16.86§	3			

*Reference numbers in parentheses.

†Based on heat of fusion of D₂O of 1515 cal/mol.

‡Indirect value (see text).

§Present result from the density measurement method.

ture measured under the saturated vapor pressure of the hydrate is therefore a true "critical decomposition temperature", a result probably generally true of all simple structure II hydrates which decompose to give liquids. On the other hand, acetone hydrate decomposes to ice (and relatively acetone-rich liquid) at its incongruent melting point (8), which may be expected to rise somewhat with the application of pressure.

Compositions of Structure II Hydrates

Table 3 gives the results of earlier composition studies of structure II hydrates. The second and third columns show, respectively, the molar heats of decomposition into liquid water and gaseous hydrate-former and into ice I and gaseous hydrate-former, as derived from the dependence of pressure on temperature along the respective three-phase equilibrium lines. The difference between these heats at 0 °C is $n\Delta H(I \rightarrow l_1)$ (28). The value *n* so obtained, with the heat of fusion of ice taken as 1435.7 cal/mol, is given in column 4. These values of *n* vary greatly in accuracy, not only with the number and accuracy of the original data, but also with the adequacy of the corrections made for gas imperfection, the presence of water vapor in the gas, and the effect of finite solubility of hydrate-former in water. Only Glew (29) appears to have combined accurate measurements with a proper statistical

study of the errors. We have attempted to represent the relative accuracy of individual values of *n* in terms of weights (*w*) assigned on a scale of 0 to 4.

Values of *n* in column 6 were derived from the shift of the h-l₁-g equilibrium produced by addition of NaCl, according to the method of Miller and Strong (30). The values in the final column are the results of various attempts at direct analysis and are generally of lower accuracy. An exception is the analysis of chloroform hydrate by Barrer and Ruzicka (31) who found the large cages to be 94 to 98% occupied by chloroform with measurements made in the presence of various "help gases".

Consideration of these results suggests that in no case has a statistically significant departure from the ideal composition of *n* = 17 been demonstrated. Certainly this is true of the results as a whole. With cases of *w* = 0 omitted, the unweighted mean of the values of *n* in columns 4 and 6 is 16.99 ± 0.54 . More realistically, weighting according to *w*² gives 17.01 ± 0.31 . Thus at about the 85% level of confidence, more than 98% of the large cages are occupied.

We conclude that the available composition data for structure II hydrates are of insufficient accuracy to test the extent of applicability of the relation between the μ -potential of water in equilibrium with the clathrate (μ_1) and that of

the empty lattice (μ_1^0),

$$[12] \quad \mu_1 = \mu_1^0 + \frac{kT}{17} \ln \left(1 - \frac{17}{n} \right)$$

given by the ideal solid solution theory (32). Equation 12 predicts an invariable composition for these hydrates in equilibrium with ice at a fixed temperature and pressure and gives $(\mu_1^0 - \mu_1) > 125$ cal/mol for more than 98% occupancy of the cages at 0 °C.

We are greatly indebted to R. E. Hawkins for technical assistance.

1. M. VON STACKELBERG and H. R. MÜLLER. *Z. Elektrochem.* **58**, 25 (1954).
2. M. VON STACKELBERG and B. MEUTHEN. *Z. Elektrochem.* **62**, 130 (1958).
3. R. K. MACMULLAN and G. A. JEFFREY. *J. Chem. Phys.* **42**, 2725 (1965).
4. R. E. HAWKINS and D. W. DAVIDSON. *J. Phys. Chem.* **70**, 1889 (1966).
5. D. F. SARGENT and L. D. CALVERT. *J. Phys. Chem.* **70**, 2689 (1966).
6. A. S. QUIST and H. S. FRANK. *J. Phys. Chem.* **65**, 560 (1961).
7. G. J. WILSON and D. W. DAVIDSON. *Can. J. Chem.* **41**, 264 (1963).
8. B. MORRIS and D. W. DAVIDSON. *Can. J. Chem.* **49**, 1243 (1971).
9. D. N. GLEW and N. S. RATH. *J. Chem. Phys.* **44**, 1710 (1966).
10. H. A. PALMER. Thesis. University of Oklahoma. 1950.
11. J. ERVA. *Suomen Kemistil.* **29B**, 183 (1956).
12. K. L. PINDER. *Can. J. Chem. Eng.* **43**, 271, 274 (1965).
13. M. VON STACKELBERG. *Naturwiss.* **36**, 327, 359 (1949).
14. S. R. GOUGH and D. W. DAVIDSON. *J. Chem. Phys.* **52**, 5442 (1970).
15. I. KIRSHENBAUM. Physical properties and analysis of heavy water. McGraw-Hill Book Co., Inc., New York. 1951. p. 6.
16. G. WADA and S. UMEDA. *Bull. Chem. Soc. Japan*, **35**, 1797 (1962).
17. P. W. BRIDGMAN. *Proc. Am. Acad. Arts Sci.* **47**, 441 (1912).
18. F. E. CRITCHFIELD, J. A. GIBSON, JR., and J. L. HALL. *J. Am. Chem. Soc.* **75**, 6044 (1953).
19. Landolt-Bornstein Zahlenwerte und Funktionen. Vol. IV. 6th ed. Springer-Verlag, Berlin. Part 1, p. 101.
20. M. VON STACKELBERG and W. MEINHOLD. *Z. Elektrochem.* **58**, 40 (1954).
21. J. ERVA. *Suomen Kemistil.* **28B**, 131 (1955).
22. R. CIGNA and E. SEBASTIANI. *Annali di Chim.* **54**, 1048 (1964).
23. G. TAMMANN and G. J. R. KRIGE. *Z. anorg. allgem. Chem.* **146**, 179 (1925).
24. Landolt-Bornstein Zahlenwerte und Funktionen. Vol. II. Part 2b, p. 3-400.
25. J. TIMMERMANS. *Proc. Roy. Soc. Dublin*, **13**, 327 (1912).
26. M. VON STACKELBERG and W. JAHNS. *Z. Elektrochem.* **58**, 162 (1954).
27. G. CHANCEL and F. PARMENTIER. *Compt. rend.* **100**, 27 (1885).
28. F. E. C. SCHEFFER and G. MEYER. *Proc. Roy. Acad. Sci. Amsterdam*, **21**, 1204 (1919); **21**, 1338 (1919).
29. D. N. GLEW. *Can. J. Chem.* **38**, 208 (1960).
30. B. MILLER and E. R. STRONG, JR. *Am. Gas Assoc. Monthly*, **28**, No. 2, 63 (1946).
31. R. M. BARRER and D. J. RUZICKA. *Trans. Faraday Soc.* **58**, 2239 (1962).
32. J. H. VAN DER WAALS and J. C. PLATTEEUW. *Adv. Chem. Phys.* **2**, 1 (1959).
33. L. D. SORTLAND and D. B. ROBINSON. *Can. J. Chem. Eng.* **42**, 38 (1964).
34. D. R. HAFEMANN and S. L. MILLER. *J. Phys. Chem.* **73**, 1392 (1969).
35. D. R. HAFEMANN and S. L. MILLER. *J. Phys. Chem.* **73**, 1398 (1969).
36. W. M. DEATON and E. M. FROST, JR. Monograph No. 8, U.S. Bureau of Mines. 1946.
37. A. J. BARDUHN, H. E. TOWLSON, and Y. C. HU. *Am. Inst. Chem. Eng. J.* **8**, No. 2, 176 (1962).
38. P. J. CECCOTTI. *Ind. Eng. Chem. Fundam.* **5**, No. 2, 106 (1966).
39. A. J. BARDUHN, O. S. ROUHER, and D. J. FONTAGNE. U.S. Office of Saline Water, Res. Dev. Prog. Report 366, 1968.
40. T. UCHIDA and I. HAYANA. *Govt. Chem. Ind. Res. Inst. Tokyo*, **59**, 382 (1964).
41. W. P. BANKS, B. O. HESTON, and F. F. BLANKENSHIP. *J. Phys. Chem.* **58**, 962 (1954).
42. T. A. WITTSRUCK, W. S. BREY, JR., and W. H. RODEBUSH. *J. Chem. Eng. Data*, **6**, 343 (1961).
43. Syracuse Univ. Res. Inst. U.S. Office of Saline Water Res. Dev. Prog. Report, 70, 1963.
44. F. A. BRIGGS, Y. C. HU, and A. J. BARDUHN. U.S. Office of Saline Water Res. Dev. Prog. Report 59, 1962.